Thermal ideality factor of hydrogenated amorphous silicon *p-i-n* solar cells

R. Kind,[1] R. A. C. M. M. van Swaaij,[1,a)] F. A. Rubinelli,[2] S. Solntsev,[1] and M. Zeman[1]
[1]*Delft University of Technology, Photovoltaic Materials and Devices Laboratory, P. O. Box 5031, 2600 GA Delft, the Netherlands*
[2]*INTEC, CONICET, Universidad Nacional del Litoral, Güemes 3450, 3000 Santa Fe, Argentina*

(Received 15 July 2011; accepted 18 October 2011; published online 29 November 2011)

The performance of hydrogenated amorphous silicon (a-Si:H) *p-i-n* solar cells is limited, as they contain a relatively high concentration of defects. The dark current voltage (JV) characteristics at low forward voltages of these devices are dominated by recombination processes. The recombination rate depends on the concentration of active recombination centers and the recombination efficacy of each of these centers. The first factor causes the ideality factor of the devices to be non-integer and to vary with voltage. The temperature dependence of the dark current can be expressed by its activation energy. For microcrystalline silicon solar cells the activation energy varies with voltage with a so-called thermal ideality factor of 2. This value was derived for devices with a spatially uniform defect distribution and reflects the recombination efficacy. Here we present results of a thickness series of a-Si:H *p-i-n* solar cells. We have matched the experimental curves with computer simulations, and show that the voltage-dependent ideality factor curve can be used to extract information on the cross sections for electron and hole capture. Also, the activation energy is used as a measure for the mobility gap, resulting in a mobility gap for a-Si:H of 1.69 eV. We find a thermal ideality factor close to 2 for all samples. This is explained with a theoretical derivation, followed by a comparison between the internal electric field strength and the spatial variation of the defect density in the intrinsic layer. The thermal ideality factor is shown to be insensitive to the defect distribution and the recombination profile in the device. It is, therefore, an appropriate parameter to characterize a-Si:H *p-i-n* devices, providing direct insight on the recombination efficacy. © *2011 American Institute of Physics*. [doi:10.1063/1.3662924]

I. INTRODUCTION

In view of the urgent need for sustainable sources of energy, hydrogenated amorphous silicon (a-Si:H) solar cells are promising. They have the potential to produce electricity from solar energy at a large scale and at low cost. Their production process is less material and energy intensive than the production process of conventional crystalline silicon (c-Si) solar cells, and allows for the use of a wide range of substrates. However, as a result of the abundant defects in the a-Si:H lattice, they suffer from a high recombination rate, reflected by the relatively large current under dark conditions. To make large-scale implementation of this type of solar cells feasible, the performance of the cells needs to be optimized. Therefore, a full understanding of the mechanisms that govern their operation is essential.

Various authors have studied the dark current characteristics of a-Si:H devices. They often focused on the ideality factor, in order to obtain information on the recombination characteristics.[1–5] However, in a-Si:H the ideality factor is non-integer and decreases with temperature.[1,4,5] Its varying value has been related to the shape of the continuous density of states distribution in the material[1] and to the spatial distribution of gap states.[3] A more recent publication showed that the ideality factor is not even constant with voltage, as was generally assumed.[2] Clearly, there is still no consensus in literature on the interpretation of the ideality factor and its relation to the recombination characteristics.

We contribute to the discussion with a thorough analysis of the dark current characteristics of a-Si:H *p-i-n* devices, in which we simultaneously studied the dependence of the dark current on the *i*-layer thickness and on the temperature. Subsequently, we used the simulation package ASA to simulate the operation of these devices. Considering the complex and interacting processes occurring in a-Si:H *p-i-n* devices, numerical simulations can be a useful tool to help understand their operation and determine their properties. Generally, the simulated curves are fitted to characteristic curves obtained from measurements, most importantly the spectral response curve and the current-voltage curve under dark and illuminated conditions. We show that the activation energy curve and the voltage-dependent ideality factor curve also can reveal important information on certain device properties, such as the mobility bandgap and the cross sections for electron and hole capture. Having calibrated the model we use the simulation outcomes to help explain our experimental observations.

Our approach comprises a focus on the temperature dependence of the dark current and the associated activation energy. In addition to the classic ideality factor, we discuss the concept of the thermal ideality factor, which was first introduced by Pieters *et al.* in a study on μc-Si:H devices.[6] We extend this theory to a-Si:H devices and show that the thermal ideality factor is a more appropriate parameter to characterize in a general manner the dark current

[a)]Author to whom correspondence should be addressed. Electronic mail: R.A.C.M.M.vanSwaaij@TUDelft.nl.

 © 2011 American Institute of Physics

Downloaded 31 Jan 2012 to 131.180.130.114. Redistribution subject to AIP license or copyright; see http://jap.aip.org/about/rights_and_permissions

characteristics of a-Si:H devices than the classic ideality factor. The thermal ideality factor eliminates the influence of the density of states distribution and the spatial distribution of defects, and therefore directly reflects the recombination efficacy.

II. THEORETICAL CONSIDERATIONS

Dark current-voltage (JV) characteristics of silicon diodes can be characterized by their ideality factor m, given by:

$$J(V) = J_0 \exp\left(\frac{qV}{mkT}\right). \tag{1}$$

As opposed to ideal c-Si diodes, a-Si:H diodes have a non-integer ideality factor that varies with temperature.[1,4,5] A possible explanation resides in the fact that the recombination rate depends on two factors: the concentration of active recombination centers, and the recombination efficacy of each of these recombination centers. The active recombination centers include all traps located between the quasi-Fermi levels for trapped charge.[7,8] In a-Si:H diodes not only the recombination efficacy, but also the concentration of active recombination centers varies with voltage, due to the continuous density of states in the bandgap.[1] Van Berkel *et al.*[1] derived an expression for the ideality factor, in which they accounted for the continuous density of states distribution in the mobility bandgap, assuming that this distribution is exponential in the region of interest. Elegant as it may seem, however, the derivation is based on the assumption that the active recombination centers are located between the quasi-Fermi levels for charge carriers, rather than the quasi-Fermi levels for *trapped* charge carriers. The two differ considerably from each other and can therefore not be interchanged. The quasi-Fermi levels for trapped electrons and holes, E_{fn_t} and E_{fp_t}, respectively, are given by:[7,8]

$$E_{fn_t} = E_c + kT \ln\left(\frac{R_\sigma n + p}{R_\sigma N_c}\right), \tag{2}$$

$$E_{fp_t} = E_v - kT \ln\left(\frac{R_\sigma n + p}{N_v}\right), \tag{3}$$

where E_c and E_v are the conduction and valence band edge, respectively; N_c and N_v are the effective densities of states in the conduction and valence band; n and p are the free electron and hole concentrations; and R_σ is the ratio between the cross sections for electron and hole capture. Because the quasi-Fermi levels for trapped charge vary over the width of the device and have a rather complex dependence on the applied voltage, the approach by Van Berkel *et al.*[1] does not lead to a simple analytical expression for the ideality factor.

Deng and Wronski[2] argued that the density of states in the mobility gap is a complex function of energy, rather than a simple exponential function as assumed by Van Berkel *et al.*[1] Consequently, the concentration of recombination centers is a complex function of bias voltage and the ideality factor cannot be considered independent of voltage. Instead, Deng and Wronski define a voltage-dependent ideality factor:[2]

$$m(V) = \left[\frac{kT}{q}\frac{d\ln J_D}{dV}\right]^{-1}. \tag{4}$$

The shape of the $m(V)$ curve indirectly reflects the shape of the density of states distribution in the mobility bandgap. For its interpretation Deng and Wronski[2] rely on the above-mentioned derivation by van Berkel *et al.*[1] However, taking into account that the relation Van Berkel *et al.* try to derive is in reality much more complex, the interpretation of the $m(V)$ curve is not straightforward even for constant values of $m(V)$.

Recently, a new parameter was introduced in the context of a study on μc-Si:H, defined as the *thermal* ideality factor.[6] Similarly to the ideality factor it characterizes the relation between the dark current and the voltage. While the ideality factor is derived from the current as a function of the voltage, the *thermal* ideality factor is derived from the *temperature* dependence of the current as a function of voltage. In what follows we briefly summarize the derivation of the thermal ideality factor, based on the work by Pieters *et al.*[6] Note, however, that Pieters *et al.* assume equal cross sections for electron and hole capture. We consider this assumption not very realistic, especially considering the values we use in our simulations, and eliminated it from the derivation.

The temperature dependence of a process, in this case the current density J conducted through the device, can be expressed by its activation energy, which is defined as:

$$E_a \equiv -\frac{\partial(\ln\{J[(kT)^{-1}]\})}{\partial[(kT)^{-1}]}. \tag{5}$$

Under low forward voltages, the dark current in a-Si:H *p-i-n* devices is dominated by Shockley-Read-Hall (SRH) recombination.[9,10] For the analytical derivation of the activation energy of SRH recombination[11] we neglect the recombination in the doped layers, as well as at the interfaces. This means that the total recombination rate is approximated by the recombination in the *i*-layer, integrated over the width of this layer. SRH-recombination occurs in trap states, located in the mobility bandgap. Hence, the recombination rate depends on two factors: the spatial and energetic distribution of the trap states N_t, and the recombination rate per trap state, defined as the recombination efficacy η_R. Determining the recombination efficacy according to the SRH statistics[12] and the Simmons and Taylor 0 K approximation[7,8] reveals that only trap states located between the quasi-Fermi levels for trapped charge, E_{fn_t} and E_{fp_t}, are active as recombination centers.[7,8] Hence, the total recombination rate can be expressed as:

$$R = \int_0^W v_{th}\sigma_n \frac{np}{R_\sigma n + p}\left(\int_{E_{fp_t}}^{E_{fn_t}} N_t(E_t)dE_t\right)dx, \tag{6}$$

where v_{th} is the thermal velocity; σ_n is the cross section for electron capture; and $N_t(E_t)$ is the concentration of active recombination centers. The term between brackets represents the local concentration of active recombination centers, while the other term describes the recombination efficacy.

Downloaded 31 Jan 2012 to 131.180.130.114. Redistribution subject to AIP license or copyright; see http://jap.aip.org/about/rights_and_permissions

For the sake of clarity we assume at this stage that the distribution of recombination centers is spatially uniform, so that $N_t(E_t)$ in Eq. (6) can be eliminated from the integration over x. Note that for a-Si:H devices we consider this assumption rather unrealistic. We will therefore come back to it in the discussion. Furthermore, we assume that the quasi-Fermi levels are constant in the device with respect to the potentials at the contacts, that the separation between the quasi-Fermi levels is equal to the applied voltage multiplied by the elementary charge q, and that the electric field E_0 is uniform. n and p can now be written as linear functions of position:[6]

$$n = n_0 \exp\left[-\frac{qE_0(x-x_0)}{kT}\right], \tag{7}$$

$$p = p_0 \exp\left[\frac{qE_0(x-x_0)}{kT}\right], \tag{8}$$

where n_0 and p_0 are the electron and hole concentrations, respectively, at position x_0. For convenience, x_0 is defined as the position where the term $\frac{np}{R_\sigma n+p}$ has a maximum, which is at $R_\sigma n = p$. Substituting Eqs. (7) and (8) in Eq. (6) and using $R_\sigma n_0 = p_0$ yields:

$$\begin{aligned} R &= \upsilon_{th}\sigma_n n_0 N_T \int_0^W \frac{R_\sigma^{\frac{3}{2}} \exp\left[\frac{qE_0(x-x_0)}{kT} + \ln R_\sigma^{-\frac{1}{2}}\right]}{\left\{\exp\left[\frac{qE_0(x-x_0)}{kT} + \ln R_\sigma^{-\frac{1}{2}}\right]\right\}^2 + 1} dx \\ &= \upsilon_{th}\sigma_n n_0 N_T R_\sigma^{\frac{3}{2}} \frac{kT}{qE_0} \left(\arctan\left\{\exp\left[\frac{qE_0(x-x_0)}{kT} + \ln R_\sigma^{-\frac{1}{2}}\right]\right\}\right)_{x=0}^{x=W} \\ &\approx \upsilon_{th}\sigma_n n_0 N_T R_\sigma^{\frac{3}{2}} \frac{kT}{2qE_0}\pi, \end{aligned} \tag{9}$$

where $N_T = \int_{E_{fp_t}}^{E_{fn_t}} N_t(E_t) dE_t$.

Having derived this expression for the total recombination current, we substitute it for J in Eq. (5) to determine the activation energy of the SRH recombination. We assume that the temperature dependence of the concentration of active recombination centers can be neglected in comparison with the temperature dependence of the recombination efficacy. In addition, we assume that in the region around x_0, where $R_\sigma n = p$, the separations between the quasi-Fermi levels and their respective band edges are approximately equal: $E_c - E_{fn} = E_{fp} - E_\upsilon = (E_\mu - V)/2$. Applying Eq. (5) results in the elimination of all temperature-independent terms in Eq. (9). Accounting for the temperature dependence of υ_{th} and n_0 we obtain the following expression for the activation energy of the total recombination:

$$E_a^R(V) = \frac{E_\mu - V}{2} + 3kT. \tag{10}$$

The factor 2 in this equation originates from the SRH statistics and was defined by Pieters *et al.* as the thermal ideality factor.[6]

III. EXPERIMENTAL PROCEDURE

We deposited two series of a-Si:H *p-i-n* solar cells with various *i*-layer thicknesses. The first series has the following structure: TCO/*p*-a-SiC:H/*i*-a-Si:H/*n*-a-Si:H/Al. The second series contains the same layers as the first series, but a 5-nm thick silicon carbide (a-SiC:H) buffer layer was included between the *p*- and the *i*-layer, to eliminate excessive interface recombination and boron diffusion into the *i*-layer. The a-Si:H layers were deposited on Asahi U-type substrates using plasma-enhanced chemical vapor deposition. The buffer layer was deposited using a silane-methane plasma diluted with hydrogen. In all samples the *p*- and *n*-layers have thicknesses of 10 nm and 20 nm, respectively. The *i*-layer thickness varies per sample: the cells without a buffer layer have *i*-layer thicknesses of 200, 400, 600, and 800 nm, while the ones with a buffer layer have *i*-layer thicknesses of 200, 400, 600, and 900 nm. All samples contain a 300 nm Al back contact. After depositing the cells we accurately removed the *n*-layer extending around the contacts in an Alcatel Reactive Ion Etching machine, to prevent current spreading into the *n*-layer, which could otherwise deteriorate the dark JV measurements at low bias voltages.[13]

We measured the quantum efficiency curves of our samples using a Newport system, comprising an Oriel Apex illuminator coupled to an Oriel Cornerstone 1/8 m monochromator and an Amtek 7225 lock-in amplifier. Subsequently, the current-voltage (JV) characteristics under illuminated conditions were determined with an Oriel solar simulator, which mimics the standard air mass 1.5 spectrum with an integrated power density of 100 mW/cm^2. For accurate measurements of the JV characteristics under dark conditions we used a Keithley 6517 A electrometer. A computer routine ensured that the current was stabilized before it was recorded. We noticed that the measurement direction influences the quality of the dark current measurements. Measuring from high to low voltages led to well reproducible results and was therefore selected as the approach to be followed. The dark JV curves were determined at eight temperatures ranging from 30 °C to 100 °C.

IV. RESULTS

A typical example of the dark current-voltage (JV) curves at various temperatures of one of our samples is

Downloaded 31 Jan 2012 to 131.180.130.114. Redistribution subject to AIP license or copyright; see http://jap.aip.org/about/rights_and_permissions

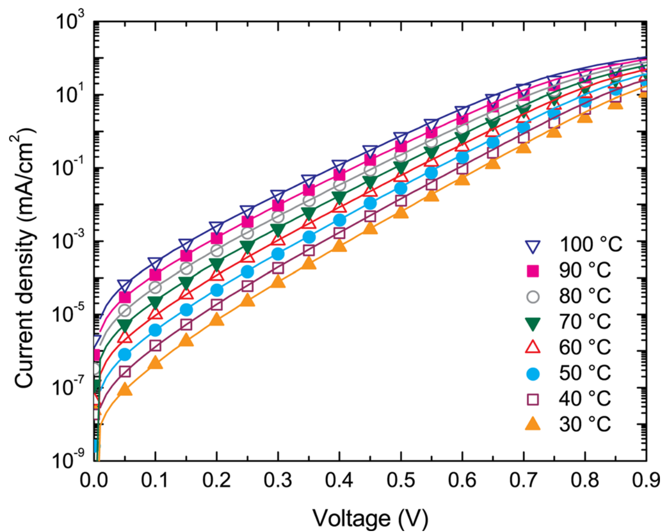

FIG. 1. (Color online) Dark current-voltage curves at various temperatures of a sample with a buffer layer and an *i*-layer thickness of 600 nm. The symbols are measurements, the lines are simulations.

shown in Fig. 1. From these curves we determined the ideality factor m according to Eq. (1), for all samples and at all temperatures. As can be seen in Fig. 2 the ideality factor increases with *i*-layer thickness and decreases with temperature. Also, the cells with a buffer layer have higher ideality factors than the cells without a buffer layer.

We used the JV curves to determine the voltage-dependent ideality factor ($m(V)$) curves of our samples, according to Eq. (4). Figure 3 shows the curves of the samples with buffer layer at 30 °C and 100 °C. The variations with voltage can be attributed to the shape of the energetic distribution of gap states, as well as the voltage dependence of the quasi-Fermi levels for trapped charge. The latter determine which gap states are active as recombination centers.[7,8] The shape of $m(V)$ versus V thus reflects, although in a rather complex manner, the density of states distribution in the mobility gap at the location where the recombination peaks. Looking at Fig. 3 we can see that $m(V)$ increases with voltage over the entire range and the curve exhibits a small bump in the region around $V = 0.5$ V. This bump is also observed in the $m(V)$ curves of the other samples. It might represent a specific feature of the density of states distribution, such as a dip in between the two peaks in the dangling bond states distribution or the onset of a considerable contribution to the recombination rate from the valence band tail states. We also see that the $m(V)$ curves are slightly dependent on the *i*-layer thickness. Because the location where the recombination peaks changes with *i*-layer thickness, this result reveals information on the spatial characteristics of the density of states distribution. If the defect distribution were to be uniform, the density of states distribution at the location where the recombination peaks would not change, even if the peak itself would be shifted. The $m(V)$ curve would therefore not be sensitive to the *i*-layer thickness. The curves in Fig. 3, however, exhibit a clear trend with thickness, indicating that the defect distribution is not uniform.

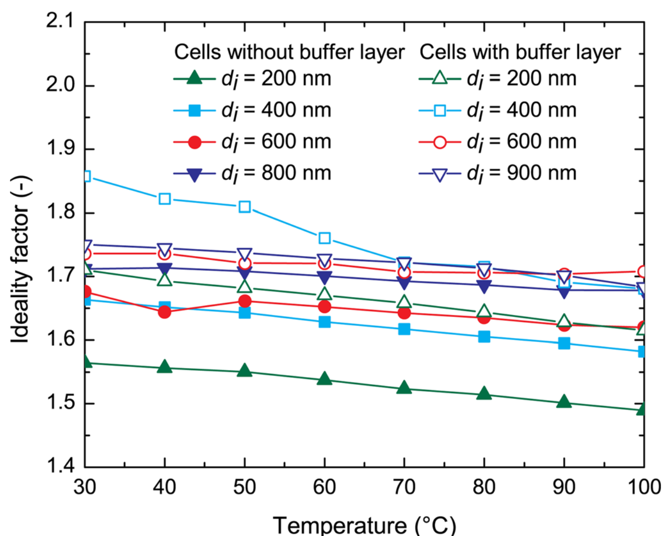

FIG. 2. (Color online) Ideality factors as a function of temperature for samples with various *i*-layer thicknesses, both with and without a buffer layer. Note that the 400 nm cell with a buffer layer has a leakage current, which explains the relatively high ideality factor at low temperatures.

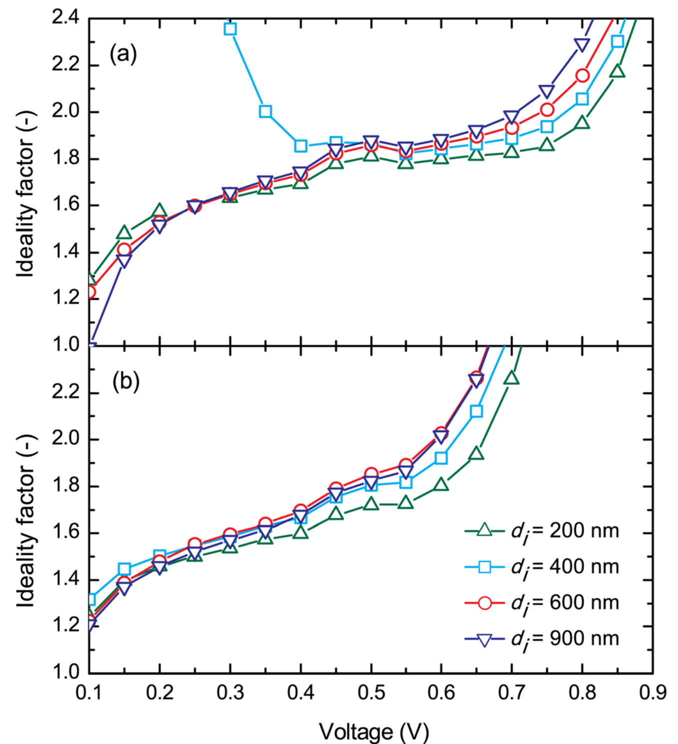

FIG. 3. (Color online) Thickness dependence of the voltage-dependent ideality factor as a function of voltage at (a) 30 °C and (b) 100 °C. The deviating curve of the 400 nm cell with a buffer layer is due to a leakage current.

Having analyzed the dark current as a function of the voltage, we now turn our attention to the temperature dependence of the current as a function of the voltage. We determined the activation energy of our samples from the experimentally obtained JV curves, according to Eq. (5). The result is shown in Fig. 4. A striking feature of this plot is that all curves seem to overlap fairly well in the voltage range between 0.2 V and 0.55 V, decreasing linearly with voltage. Apparently, in this region the activation energy is independent of the thickness of the *i*-layer and the presence of a buffer layer.

Downloaded 31 Jan 2012 to 131.180.130.114. Redistribution subject to AIP license or copyright; see http://jap.aip.org/about/rights_and_permissions

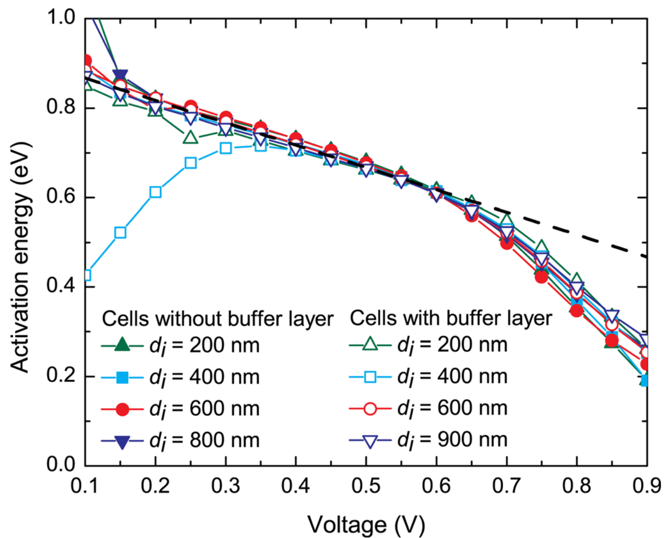

FIG. 4. (Color online) Activation energy of a-Si:H *p-i-n* devices with and without a buffer layer and with various *i*-layer thicknesses. The dashed line is a global linear least squares fit of Eq. (10) to the experimental curves, in the range from 0.2 V to 0.55 V. The leakage current in the 400 nm cell with a buffer layer results in a low activation energy at low voltages. Only the part of this curve between 0.4 V and 0.55 V was included in the global fit.

Pieters *et al.* found a similar curve for the activation energy of the dark current in μc-Si:H devices.[6] They showed that over a certain voltage range the slope of their curve corresponds to a thermal ideality factor of 2, in agreement with Eq. (10). We determined the thermal ideality factor of our samples in the voltage range between 0.2 V and 0.55 V, by replacing the factor 2 in Eq. (10) by the variable m_{th} and fitting the equation to our curves. We assumed that all samples have approximately equal thermal ideality factors. This is justified by the fact that Fig. 4 does not show a trend in activation energy with thickness, nor a significant difference between the activation energies for cells with a buffer layer and cells without a buffer layer. The assumption allowed us to make a global least-squares fit to all curves simultaneously rather than individually, thereby increasing the reliability of the fit. The result we found is a thermal ideality factor equal to 2.09 $\pm$ 0.042. This value is very close to the value of 2 predicted by Eq. (10) and therefore confirms the validity of this equation.

V. SIMULATIONS

To gain more insight on the intrinsic behavior of a-Si:H *p-i-n* devices with respect to the recombination processes, as well as to verify the analytical derivation of the activation energy, we carried out numerical simulations using the software package ASA, developed at Delft University of Technology. We used the measured quantum efficiency curves and the JV curves under dark and illuminated conditions to calibrate the numerical model. In line with our experimental analysis, we also involved the voltage-dependent ideality factor and the activation energy curve in our calibration. To increase the reliability of the calibration, all samples were simulated using a single set of parameters, ignoring any unintended deviations in material properties in the various samples. The parameter values were optimized until the model was capable of reproducing all of our measured characteristic curves to a satisfactory extent. A non-uniform defect distribution as predicted by the defect-pool model developed by Powell and Deane[14] was assumed. This allowed for reproduction of the limited dependence of the dark JV curves on the *i*-layer thickness observed in the experiments. For completeness we also ran simulations in which we adopted a uniform defect distribution, but this consistently led to a larger thickness dependence, as also was noticed by other authors.[3,15] We also tested it with another simulation package, D-AMPS, which was developed at INTEC, UNL (Universidad Nacional del Litoral) in Argentina. With this package too we were able to reproduce the curves only by applying the defect-pool model. The assumption of a uniform defect distribution was therefore rejected.

Calculation of the $m(V)$ curves associated with dark JV curves produced by simulations, revealed that the $m(V)$ curve contains features that cannot be seen well in the exponential dark JV curve. The $m(V)$ curve is very sensitive to the density of states distribution in the mobility gap, and therefore to the dangling bond and valence-band tail parameters. In addition, the capture cross sections of the different types of traps, i.e., the donor-like traps and the acceptor-like traps, as well as the traps in the valence band tail and the conduction band tail, have a large influence on $m(V)$. This is a result of the fact that the ratios between the various cross sections determine the relative contribution of the different types of traps to the recombination current. Even if the effect is hardly visible in the dark JV curve, changing the sizes of the cross sections relative to one another can affect the $m(V)$ curve considerably. The $m(V)$ curve is therefore an important reference for calibrating the model, especially for studying the energetic distribution of gap states and the cross sections of the various types of trap states. Fitting the $m(V)$ curves turned out to be rather hard, especially without deteriorating the other fitted curves, but we have been able to roughly reproduce the shapes of the experimental $m(V)$ curves. Figure 5 shows the fit of the $m(V)$ curve for the 600 nm cell with a buffer layer, as well as an illustration of the sensitivity of this curve to the dangling bond distribution and the cross section for electron capture.

Furthermore, our simulations showed that the activation energy curve is very sensitive to the mobility gap, as also predicted by Eq. (10). To match the activation energy curve we needed to adopt a mobility gap of 1.69 eV. A higher value resulted in a very poor fit, as illustrated in Fig. 6. The value of 1.69 eV is lower than values generally encountered in literature. Wronski *et al.*[16] and Lee *et al.*[17] used internal photoemission spectroscopy to determine the mobility gap and found values of 1.90 eV. Other authors reported values of 1.70 eV (Ref. 18) and 1.73 eV.[13] Later studies showed that the mobility gap is strongly dependent on the hydrogen dilution during the growth of a-Si:H,[19,20] exhibiting variations between 1.80 eV and 1.95 eV. However, these values were adjusted by Sturiale and Rubinelli after analysis of the same data using D-AMPS.[15] Their study indicated that the mobility gaps of the studied materials were actually 0.08 eV smaller, implying a mobility gap of 1.72 eV for material deposited using no hydrogen dilution. This value resembles the values

Downloaded 31 Jan 2012 to 131.180.130.114. Redistribution subject to AIP license or copyright; see http://jap.aip.org/about/rights_and_permissions

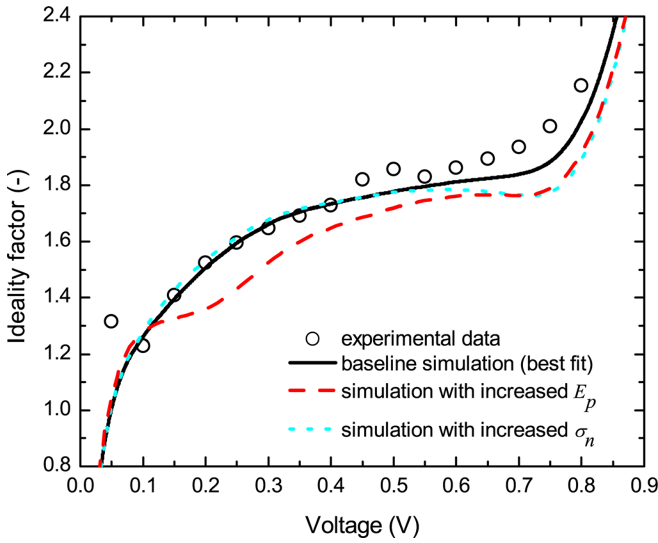

FIG. 5. (Color online) The ideality factor as a function of voltage for a cell with a buffer layer and an i-layer thickness of 600 nm, at 30 °C. The solid line is the $m(V)$ curve corresponding to the parameters in Table I. The dashed line represents the $m(V)$ curve when E_p is increased by 0.04 eV. The dotted line represents the $m(V)$ curve when the dangling-bond cross sections for electron capture (both for neutral and positively charged traps) are multiplied by a factor of 2, that is, the ratio between the cross sections for electron capture and the cross sections for hole capture is doubled.

of 1.70 eV and 1.73 eV mentioned before and is also fairly close to the value we determined in this study by considering the activation energy curve.

Overall, we were able to reproduce the curves to a large extent, as well as the trends with respect to i-layer thickness and temperature. As an example, Figs. 1 and 6 show the dark JV curves and the activation energy curve of one of our samples, as well as the curves produced by our simulations. In Table I the key parameter values corresponding to our best fit are listed.

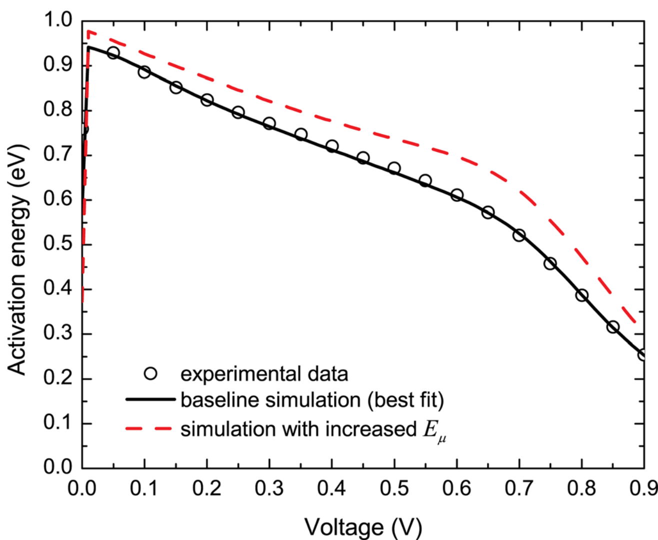

FIG. 6. (Color online) The activation energy curve of a sample with a buffer layer and with an i-layer thickness of 600 nm. The symbols represent the experimental activation energy, while the lines are simulations. The solid line corresponds to the parameter values listed in Table I (using $E_\mu = 1.69$ eV). In the simulation represented by the dashed line the mobility gap was increased to 1.8 eV, while the electron affinity was adjusted to keep the band offsets in the valence band and the conduction bands equal.

TABLE I. Key parameter values used for simulations in ASA, obtained from calibrating the model to experimental curves. E_μ is the mobility gap; N_v and N_c are the density of states in the valence and conduction band, respectively; μ_n and μ_p are the electron and hole mobilities; N_{c0}, and N_{v0} are the densities of states at the conduction and valence band edge, respectively; E_{c0}, and E_{v0} are the characteristic energies of the conduction and valence band tail, respectively; and $\sigma_{n/p}^{+/0/-}$ is the cross section for electron (n) or hole (p) capture, of a positively charged (+), neutral (0), or negatively charged (−) gap state, where we distinguish between tail states and dangling bond states; E_p and σ_{db} are defect-pool parameters.

Parameter	Value
E_μ	1.69 eV
N_v	2.0×10^{20} cm^{-3}
N_c	2.0×10^{20} cm^{-3}
μ_n	40 cm^2 V^{-1} s^{-1}
μ_p	4 cm^2 V^{-1} s^{-1}
N_{v0}	3.0×10^{21} cm^{-3} eV^{-1}
N_{c0}	1.0×10^{21} cm^{-3} eV^{-1}
E_{v0}	0.044 eV
E_{c0}	0.028 eV
$\sigma^0_{p,tails}$	1.0×10^{-18} cm^2
$\sigma^+_{n,tails}$	1.0×10^{-16} cm^2
$\sigma^0_{n,tails}$	1.0×10^{-18} cm^2
$\sigma^-_{p,tails}$	1.0×10^{-16} cm^2
E_p	1.10 eV
σ_{db}	0.160 cm^2
$\sigma^0_{p,db}$	4.0×10^{-17} cm^2
$\sigma^+_{n,db}$	8.0×10^{-15} cm^2
$\sigma^0_{n,db}$	8.0×10^{-17} cm^2
$\sigma^-_{p,db}$	2.0×10^{-15} cm^2

VI. DISCUSSION

We have seen that the ideality factors of our a-Si:H samples vary with i-layer thickness, temperature, and voltage. The *thermal* ideality factor, on the other hand, is virtually constant and close to 2 for all samples and under various conditions, in agreement with Eq. (10). Although μc-Si:H devices were already shown to obey Eq. (10),[6] the validity of the equation for a-Si:H devices is quite remarkable.

Eq. (10) was derived under the assumption of a uniform defect distribution. Pieters *et al.* argue that the equation is only valid if the spatial variation in defect density is small compared to the spatial variation in recombination efficacy.[6] If the defect distribution were not spatially uniform, a significant part of the recombination could take place close to the interfaces, e.g. the p/i interface. In this region, Pieters *et al.* reason, the quasi-Fermi level for holes is more or less fixed so that $E_c - E_{fn} \approx E_\mu - V$, leading to a thermal ideality factor close to 1.[6] Following this reasoning, the value around 2 that we found for our samples, would imply that recombination takes place in the bulk of the device, where $E_c - E_{fn} = E_{fp} - E_v$.

Yet, evidence is growing that in a-Si:H devices the defect distribution is spatially non-uniform, and highest close to the interfaces.[3,15,21] As a consequence, the recombination rate is expected to exhibit a peak close to the p/i interface, which is confirmed by our simulations. Kroon and Van

Downloaded 31 Jan 2012 to 131.180.130.114. Redistribution subject to AIP license or copyright; see http://jap.aip.org/about/rights_and_permissions

Swaaij also showed this, and propose that the fact that in this region $E_c - E_{fn} \neq E_{fp} - E_v$ is the cause of the non-integer ideality factor.[3] Clearly, there seems to be a contradiction between the theory of Pieters *et al.*[6] on the one hand, and the results found by Kroon and van Swaaij and our current results on the other hand.

An even more fundamental problem with the theory from Pieters *et al.*[6] when applied on a-Si:H devices originates from an earlier stage in the derivation. The defect distribution was assumed to be uniform, so that it could be eliminated from the integration in Eq. (6). Because we consider this assumption invalid, the derivation is not correct. To understand why our samples still seem to obey the theory, we need to incorporate the non-uniform defect distribution into the derivation of the thermal ideality factor. We assume that the spatial distribution of recombination centers is exponential, described by:

$$\int_{E_{fp_t}}^{E_{fn_t}} N_t dE_t = c_1 \exp(-c_2 x), \tag{11}$$

where c_1 and c_2 are constants. In reality, no analytical expression exists for the distribution of recombination centers. Yet, as we will see later, this highly simplified equation serves well to make an estimation of the *local* spatial variation in concentration of active recombination centers. Substituting Eq. (11) in Eq. (6) yields the following expression for the recombination rate:

$$R = \int_0^W v_{th}\sigma_n \frac{np}{R_\sigma n + p} c_1 \exp(-c_2 x) dx = v_{th}\sigma_n c_1 \int_0^W \frac{R_\sigma n_0 \exp(-c_2 x)}{\frac{1}{R_\sigma}\exp\left[\frac{qE_0(x-x_0)}{kT}\right] + \exp\left[\frac{-qE_0(x-x_0)}{kT}\right]} dx$$

$$= v_{th}\sigma_n n_0 c_1 \int_0^W \frac{R_\sigma^{\frac{3}{2}} \exp\left[-\frac{qE_0 x_0}{kT} + \left(\frac{qE_0}{kT} - c_2\right)x + \ln R_\sigma^{-\frac{1}{2}}\right]}{\left\{\exp\left[\frac{qE_0(x-x_0)}{kT} + \ln R_\sigma^{-\frac{1}{2}}\right]\right\}^2 + 1} dx. \tag{12}$$

This equation does not have a straightforward solution. Close investigation of the equation shows, however, that if $(qE_0)/(kT) \gg c_2$, the equation reduces to Eq. (9). To verify whether this condition is indeed fulfilled we use the data generated by our simulations, as described previously. The distribution of active recombination centers can be determined from the defect distribution (which in our simulations was determined according to the defect-pool model) and the quasi-Fermi levels for trapped charge. The resulting distribution for a cell with an *i*-layer thickness of 600 nm under a bias voltage of 0.4 V is shown in Fig. 7. The electric-field distribution in this cell under the same conditions is plotted in this figure. The electric field is lowest in the region around $x = 260$ nm and does not drop below 10^3 V/cm. Fitting Eq. (11) to the distribution curve of active recombination centers in this region yields $c_2 \approx 1.4 \times 10^{-6}\,\text{cm}^{-1}$. In the region close to the *p*/*i* interface, where the spatial variation of active recombination centers is largest, the fit yields $c_2 \approx 0.09\,\text{cm}^{-1}$, whereas the electric field in this region is not higher than 10^5 V/cm. Hence, the condition is fulfilled and the spatial variation in the defect density can be neglected for the derivation of the activation energy.

From these results we can conclude that the activation energy is virtually insensitive to the defect distribution, and insensitive to the location where most recombination occurs. The thermal ideality factor depends on the separations between the quasi-Fermi levels and their respective band edges in the region around x_0, which is defined as the location where $R_\sigma n = p$. At this location the recombination efficacy reaches its maximum, irrespective of the location where the recombination peaks. If at x_0 the separations between the quasi-Fermi levels and their respective band edges are equal, the thermal ideality factor will be 2. The band diagram in Fig. 8 shows that when a voltage is applied, the separations are indeed approximately equal over a large part of the device.

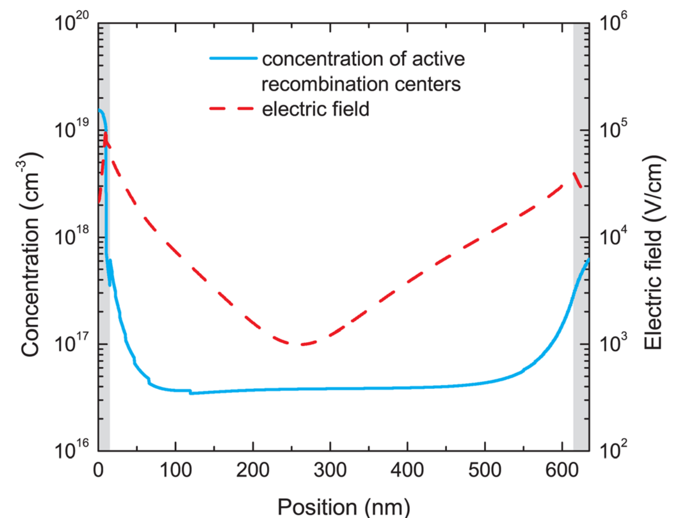

FIG. 7. (Color online) Spatial distribution of the active recombination centers (solid line) and the electric field distribution (dashed line) in an a-Si:H *p-i-n* device with a buffer layer and an *i*-layer thickness of 600 nm, under an applied voltage of 0.4 V. Both distributions were obtained from our numerical simulations. The distribution of active recombination centers was determined from the defect distribution according to the defect-pool model and the quasi-Fermi levels for trapped charge. All defects located between the quasi-Fermi levels for trapped charge were assumed to be active as recombination centers. The gray areas in the plot represent the doped layers.

Downloaded 31 Jan 2012 to 131.180.130.114. Redistribution subject to AIP license or copyright; see http://jap.aip.org/about/rights_and_permissions

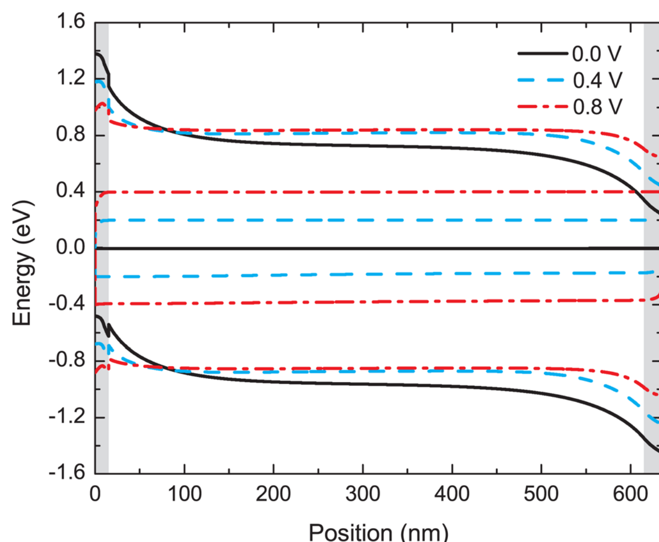

FIG. 8. (Color online) Band diagram of a cell with an *i*-layer thickness of 600 nm, at a temperature of 295 K and at various bias voltages, as predicted by simulations. The gray areas in the plot represent the doped layers.

VII. CONCLUSIONS

We have studied two concepts that can be used to characterize a-Si:H devices, i.e., the ideality factor and the thermal ideality factor. The ideality factor is related to the voltage dependence of the dark current. For a-Si:H devices it is non-integer and varies with *i*-layer thickness, temperature, and even with voltage. The voltage-dependent ideality factor can be used in simulation studies to increase the reliability of the calibration. Moreover, it can reveal information on the density of states distribution in the mobility gap as well as the relative contribution to the recombination current of the various types of trap states.

The thermal ideality factor is related to the voltage dependence of the activation energy. That is, it concerns the *temperature* dependence of the dark current rather than the dark current itself. Our work indicates that a-Si:H *p-i-n* devices exhibit a thermal ideality factor close to 2, irrespective of the precise device structure. The thermal ideality factor is insensitive to the defect distribution and the recombination profile in the device. It is therefore a more robust parameter to characterize in a general way the dark current in a-Si:H devices than the classic ideality factor. The value of 2 originates from the mechanism that dominates the recombination, i.e., Shockley-Read-Hall recombination.

As a result of the non-uniform defect distribution in a-Si:H devices, the location in the device where the recombination rate peaks does not coincide with the location where the recombination efficacy reaches its maximum. This affects the ideality factor, but does not affect the thermal ideality factor. While the ideality factor is influenced by both the recombination efficacy and the defect distribution, the thermal ideality factor depends on the recombination efficacy only. It therefore provides direct insight into the recombination efficacy, without being obscured by conditions such as temperature and voltage—which influence the concentration of defects that are active as recombination centers—or the defect distribution.

ACKNOWLEDGMENTS

We would like to thank Martijn Tijssen, Stefaan Heirman, Kasper Zwetsloot, and Jan Chris Staalenburg for the fabrication of the samples, as well as their technical assistance during the measurements. Bart Pieters is acknowledged for sharing his ideas on the interpretation of the thermal ideality factor.

[1]C. van Berkel, M. J. Powell, A. R. Franklin, and I. D. French, J. Appl. Phys. **73**, 5264 (1993).
[2]J. Deng and C. R. Wronski, J. Appl. Phys. **98**, 024509 (2005).
[3]M. A. Kroon and R. A. C. M. M. van Swaaij, J. Appl. Phys. **90**, 994 (2001).
[4]H. Matsuura, A. Matsuda, H. Okushi, and K. Tanaka, J. Appl. Phys. **58**, 1578 (1985).
[5]A. Mittiga, P. Fiorini, M. Falconieri, and F. Evangelisti, J. Appl. Phys. **66**, 2667 (1989).
[6]B. E. Pieters, H. Stiebig, M. Zeman, and R. A. C. M. M. van Swaaij, J. Appl. Phys. **105**, 044502 (2009).
[7]J. G. Simmons and G. W. Taylor, Phys. Rev. B **4**, 502 (1971).
[8]G. W. Taylor and J. G. Simmons, J. Non-Cryst. Solids **8–10**, 940 (1972).
[9]R. A. Street, J. Non-Cryst. Solids **164–166**, 643 (1993).
[10]F. A. Rubinelli, J. K. Arch, and S. J. Fonash, J. Appl. Phys. **72**, 1621 (1992).
[11]Pieters *et al.* speak about the activation energy of a *p-i-n* device. Because activation energy is by definition associated with a process, we prefer to use the term activation energy of the total SRH recombination.
[12]W. Shockley and W. T. Read, Phys. Rev. **87**, 835 (1952).
[13]J. A. Willemen, "Modelling of amorphous silicon single- and multi-junction solar cells," Ph.D. dissertation (Delft University of Technology, 1998).
[14]M. J. Powell and S. C. Deane, Phys. Rev. B **53**, 10121 (1996).
[15]A. Sturiale and F. A. Rubinelli, Thin Solid Films **516**, 7708 (2008).
[16]C. R. Wronski, S. Lee, M. Hicks, and S. Kumar, Phys. Rev. Lett. **63**, 1420 (1989).
[17]S. Lee, J. K. Arch, S. J. Fonash, and C. R. Wronski, in *Conference Record of the Twenty First IEEE Photovoltaic Specialists Conference, 1990* (IEEE, New York, 1990), Vol. 2, pp. 1624–1629.
[18]M. Zeman, J. A. Willemen, S. Solntsev, and J. W. Metselaar, Sol. Energy Mater. Sol. Cells **34**, 557 (1994).
[19]J. Deng, J. M. Pearce, R. J. Koval, V. Vlahos, R. W. Collins, and C. R. Wronski, Appl. Phys. Lett. **82**, 3023 (2003).
[20]R. J. Koval, A. S. Ferlauto, J. M. Pearce, R. W. Collins, and C. R. Wronski, J. Non-Cryst. Solids **299–302**, 1136 (2002).
[21]E. Klimovsky, A. Sturiale, and F. A. Rubinelli, Thin Solid Films **515**, 4826 (2007).

Downloaded 31 Jan 2012 to 131.180.130.114. Redistribution subject to AIP license or copyright; see http://jap.aip.org/about/rights_and_permissions